Experimental Heat Transfer Investigation Around the Film-Cooled Leading Edge of a High-Pressure Gas Turbine Rotor Blade

C. Camci

T. Arts

von Karman Institute for Fluid Dynamics, B-1640 Rhode Saint Genèse, Belgium

This paper describes an experimental heat transfer investigation around the leading edge of a high-pressure film-cooled gas turbine rotor blade. The measurements were performed in the VKI isentropic compression tube facility using platinum thin film gauges painted on a blade made of machinable glass ceramic. Free stream to wall temperature ratio, Reynolds, and Mach numbers were selected from actual aeroengines conditions. Heat transfer data obtained without and with film cooling in a stationary frame are presented. The effects of coolant to free-stream mass weight ratio and temperature ratio were successively investigated. Heat transfer modifications due to incidence angle variations were interpreted wih the aid of inviscid flow calculation methods.

Introduction

A classic way to improve the thermal efficiency of a gas turbine cycle is to increase the turbine entry temperature. As a result, specific fuel consumption, size, and weight of aeroengines were significantly reduced during the two last decades. A 25/1 pressure ratio and an 1800 K TET are typical values encountered in high-performance jet engines [1]. An accurate knowledge of the convective heat flow across the blade surfaces is therefore an important, even essential, part of their design. The stagnation point of a turbine blade is probably the most critical area as it is exposed to an important level of heat flux. Considering the ever increasing temperature and pressure levels, external film cooling coupled with internal convective and impingement cooling have been a general practice in this portion of the blade. From a fluid dynamic point of view, the regions affected by film cooling, especially very close to the ejection holes, are characterized by a flow which is viscous, obviously nonadiabatic, and fully three dimensional. The coolant jets, interacting with the boundary layer, considerably alter its initial structure.

The objective of this paper is to present detailed heat transfer data measured around the film-cooled leading edge of a high-pressure turbine rotor blade in the VKI short-duration isentropic compression tube. In the high-speed, compressible flow environment of this facility, wall heat flux measurements were performed duplicating the same Reynolds and Mach numbers as well as wall to free stream and coolant to free stream temperature ratios existing in an aeroengine. Measurement results are presented as heat transfer coefficient distributions. The effects of incidence angle, coolant to free stream mass weight ratio and coolant to free stream temperature ratio were successively investigated.

Contributed by the Gas Turbine Division of THE AMERICAN SOCIETY OF MECHANICAL ENGINEERS for presentation at the 30th International Gas Turbine Conference and Exhibit, Houston, Texas, March 18-21, 1985. Manuscript received at ASME Headquarters, December 27, 1984. Paper No. 85-GT-114.

Copies will be available until December 1985.

Experimental Apparatus

Test Facility. Short-duration testing techniques were employed; they were provided by the VKI isentropic compression tube facility. The latter consists of a 5-m-long and 1-m-dia cylinder containing a light weight piston, driven by a 250 bar air reservoir. As the piston moves, the gas in front of it is nearly isentropically compressed until it reaches a preset pressure, and hence temperature level. A fast-opening valve is then actuated, allowing the mainstream to flow through the test section until the piston has completed its stroke. The free-stream conditions may be varied between 300 and 600 K and between 0.5 and 7 bar. A 5 m^3 dump tank allows downstream pressure adjustments between 0.1 and 3 bar. Testing time is about 500 ms. Further details about this facility and its operating principles are described in [2, 3].

The Model. All measurememts reported in this paper were carried out on the same rotor blade section as tested by Consigny and Richards [4]. The cascade geometry is fully described in this reference and summarized in Fig. 1. The blade instrumented for heat flux measurements was milled from "Macor" glass ceramic and 45 platinum thin films were painted on its surface. Three rows of cooling holes (d = 0.8 mm) are located around the leading edge; the row and hole spacing are both 2.48 mm. The hole axes are spanwise inclined at 30 deg from the tangential direction. A circular cavity (ϕ = 4.5 mm) drilled along the blade height acts as an injection plenum. A regenerative type of heat exchanger provides cooling air temperatures ranging between −120°C and +150°C. Pressure tappings and miniature thermocouples provide continuously the coolant characteristics at the plenum inlet and outlet.

Discussion on this paper will be accepted at ASME Headquarters until July 15, 1985

Table 1

RUN	$P_{0\infty}$	$T_{0\infty}$	$T_w/T_{0\infty}$	$T_c/T_{0\infty}$	P_{oc}	$\dot{m}_c/\dot{m}_\infty$	Ma_{inlet}	$Ma_{exit,s}$	$Re_{\bar{c}_{inlet}}$	TU_∞	i
	b	K			b	%				%	deg.
126	2.915	410.0	0.736				.240	.901	8.40 E5	5.2	0
112	2.901	409.2	0.724				.251	.905	8.42 E5	5.2	0
113	2.905	409.4	0.727				.251	.908	8.42 E5	5.2	0
187	3.330	409.2	0.719				.251	.923	9.65 E5	5.2	0
196	3.045	417.6	0.716				.316	.951	10.66 E5	0.8	+15
198	3.040	417.8	0.713				.310	.948	10.25 E5	0.8	+10
201	3.050	417.2	0.700				.271	.952	9.27 E5	0.8	0
206	3.050	417.9	0.706				.263	.945	8.99 E5	0.8	-10
202	2.885	417.3	0.705	.39	3.72	.87	.271	.952	9.27 E5	0.8	0
199	2.902	418.3	0.710	.39	3.65	.84	.310	.948	10.25 E5	0.8	+10
204	2.892	417.8	0.707	.38	3.69	.89	.263	.945	8.99 E5	0.8	-10
154	2.883	408.9	0.722	.52	3.28	.50	.251	.905	8.42 E5	5.2	0
155	2.895	409.5	0.727	.52	3.40	.62	.251	.905	8.42 E5	5.2	0
157	2.891	409.3	0.731	.49	3.92	1.01	.251	.905	8.42 E5	5.2	0
120	2.926	410.3	0.727	.59	4.02	.57	.251	.905	8.42 E5	5.2	0
125	2.892	409.3	0.735	.59	3.73	.46	.251	.905	8.42 E5	5.2	0
130	2.862	406.5	0.722	.70	3.69	.50	.251	.905	8.42 E5	5.2	0

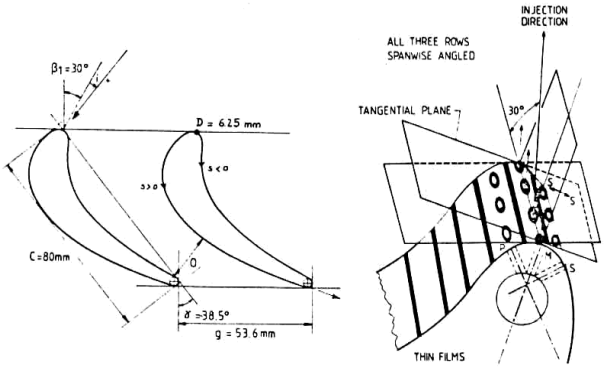

Fig. 1 Cascade geometry and cooling configuration

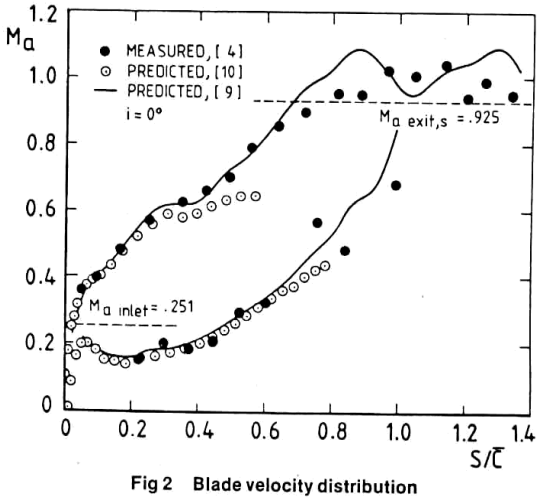

Fig 2 Blade velocity distribution

Turbulence Generation. The free-stream turbulence is generated by an upstream horizontal grid of parallel bars. The maximum turbulence level is 5.2 percent when the grid is installed at one chord length upstream of the model [4], but can be reduced by displacing the grid further upstream.

Measurement Technique. The local wall heat flux is deduced from the corresponding time dependent surface temperature evolution; the latter is obtained from platinum thin films (variable resistance thermometers) deposited on the surface. The temperature/wall heat flux conversion is obtained from an electrical analogy, simulating a semi-infinite body configuration. A detailed description of this transient technique is given in [5, 6]. The convective heat transfer coefficient is defined as the ratio of the measured wall heat flux over the difference between the free-stream recovery and local wall temperatures; a recovery factor of 0.896 is used [7] as if the boundary layer were turbulent everywhere on the blade surface. Local temperature of the wall is evaluated from measured thin film resistance, just before the mainstram flow establishment, taking into account near hole conduction effects because of slightly early start-up of injection process (~200 ms).

The uncertainties on the different measurements were estimated as following [8]:

Nomenclature

$\bar{c}$ = chord length
$\overline{C_d}$ = averaged discharge coefficient
d = ejection hole diameter
g = pitch
h_0, h = convective heat transfer coefficient, without/with film cooling
i = incidence angle (positive in the counterclockwise direction)
$\dot{m}$ = mass flow rate
m = blowing rate, $m = \rho_c U_c / \pi_\infty U_\infty$
M = leading edge midrow of ejection ($s/\bar{c} = 0.0$)
Ma = local Mach number
O = throat
p = pressure
P = leading edge pressure side row of ejection ($s/\bar{c} = -0.026$)
$\dot{q}$ = wall heat flux rate
Re = Reynolds number
s = curvilinear coordinate along the blade
S = leading edge suction side row of ejection ($s/c = +0.026$)
T = temperature
TET = turbine entry temperature
TU = turbulence intensity
U = velocity
ρ = density
γ = stagger angle

Subscripts

c = relative to coolant
d = based on injection hole diameter
D = based on leading edge diameter
o = total condition
∞ = relative to free stream
oc = plenum chamber condition
r = recovery
s = isentropic
T = based on plenum chamber diameter

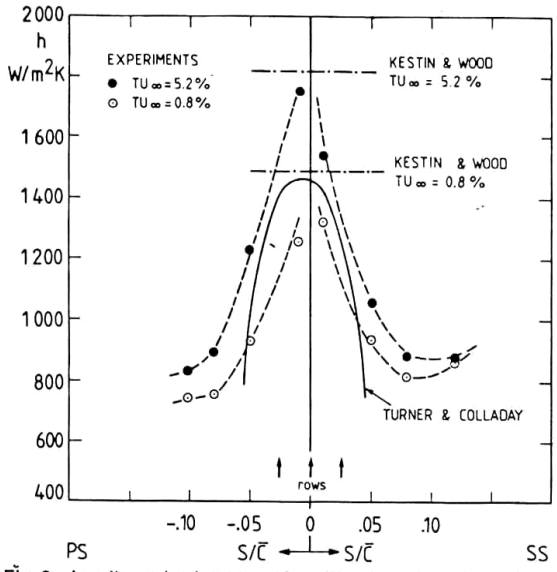

Fig. 3 Leading-edge heat transfer without cooling effect of TU_∞

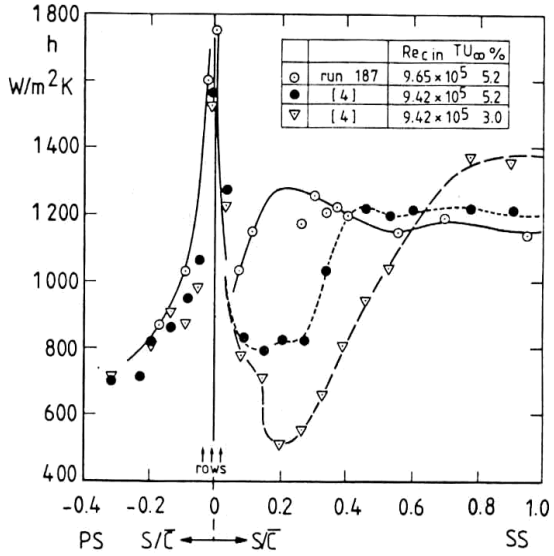

Fig. 4 Leading-edge heat transfer without cooling effect of holes' existence

$$
\begin{aligned}
h &= 1000\ \mathrm{W/m^2K} \pm 50\ \mathrm{W/m^2K}\ (\text{excluding } s/\bar{c} = \mp 0.01 \text{ with cooling}) \\
p &= 2200\ \mathrm{mm\ Hg} \pm 15\ \mathrm{mm\ Hg} \\
T &= 100\ \mathrm{K} \pm 0.5\ \mathrm{K} \\
\dot{m}_c &= 0.020\ \mathrm{kg/s} \pm 0.0005\ \mathrm{kg/s} \\
\dot{m}_c/\dot{m}_\infty &= 2 \pm 0.1\%
\end{aligned}
$$

Experimental Results and Discussion

The heat transfer behavior around the leading edge of a film-cooled rotor blade has been experimentally investigated over a range of coolant temperatures, coolant to free-stream mass weight ratios and incidence angles. The main parameters of this experimental program are summarized in Table 1.

Blade Velocity Distribution. Measured isentropic Mach number distributions around the blade are shown in Fig. 2 at zero incidence. The free-stream inlet Mach number was measured to be 0.251. Because of the relatively small leading edge radius, detailed static pressure measurements near the stagnation point could not be carried out. The flow accelerates quite regularly on the suction side up to nearly sonic conditions at the trailng edge. Along the pressure side, a velocity peak appears at $s/\bar{c} = -0.08$. More downstream, a favorable pressure gradient accelerates the flow up to the trailing edge.

A two-dimensional time marching method [9] provided an inviscid prediction of the mainstream flow (Fig. 2). Because of the weakness of this kind of approach to accurately model a very low velocity region, a singularity method [10] was also applied around the leading edge in order to carefully determine the stagnation point position. At $i = 0$, the latter was calculated to be at $s/\bar{c} = -0.019$ (Fig. 5 – point B), very close to the midrow of holes. This suggests that when no coolant is ejected, rows M and S may be considered as roughness elements for the suction side boundary layer. On the pressure side, the boundary layer is only affected by row P.

Leading-Edge Heat Transfer Without Film Cooling ($i = 0$ deg). Heat transfer coefficient distributions without coolant ejection are shown in Fig. 3 for $-0.10 < s/\bar{c} < +0.10$. In order to avoid any possible free-stream air circulation between rows M, P, and S, the coolant plenum chamber was filled with a flexible insert. In the absence of the latter, as has been demonstrated from surface oil flow visualizations, free-strean air penetrates in the plenum through row M and depending on the local static pressure, is ejected through rows P and S, affecting the local heat flux measurement.

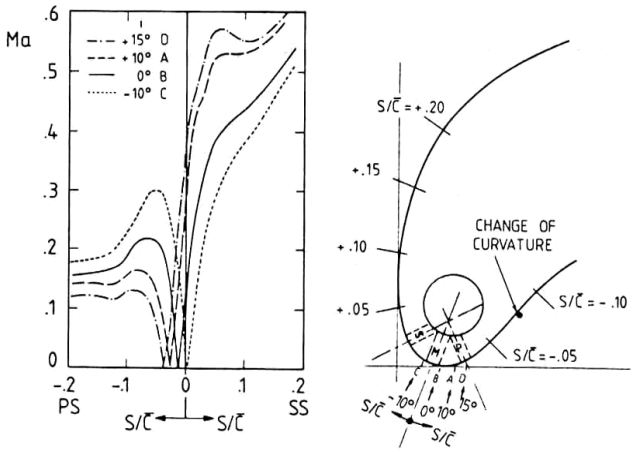

Fig. 5 Leading-edge velocity distribution effect of incidence

Stagnation region heat transfer on a cylinder in crossflow is mainly dominated by a three-dimensional vortical structure [11]. These vortices have their vorticity axes parallel to the main flow, as visualized by [12]. The amount of heat transfer is proportional to the quantity $TU_\infty \mathrm{Re}^{1/2}$. Any increase of this product decreases the spacing of these vortices and, hence, enhances heat transfer. Looking at the gauges located at $s/\bar{c} = \mp 0.01$ (Fig. 3), enhancement of heat flux is clearly observed when TU_∞ is increased from 0.8 to 5.2 percent. Kestin and Wood's cylinder in crossflow correlation [13] provides similar trends. For $TU_\infty = 0.8$ percent, the present data are also compared with Turner and Collady's cylinder in crossflow correlation [14, 15]. However, even at $i = 0$ deg, a smooth cylinder in crossflow is not an exact simulation of a turbine blade leading edge, because different accelerations exist on both sides of the stagnation line. Moreover, the present model displays three rows of holes acting as roughness elements.

The heat transfer distributions are affected by the existence of these holes, even when no coolant is ejected. This was demonstrated by comparing the present measurements with those by Consigny and Richards [4], performed on an identical, but smooth profile (Fig. 4). On the pressure side, at $TU_\infty = 5.2$ percent, nearly similar heat transfer levels were observed. The effect of the holes is not very pronounced. As a matter of fact, the boundary layer transition is mainly due to the curvature change, at $s/\bar{c} = -0.08$, where the breakdown

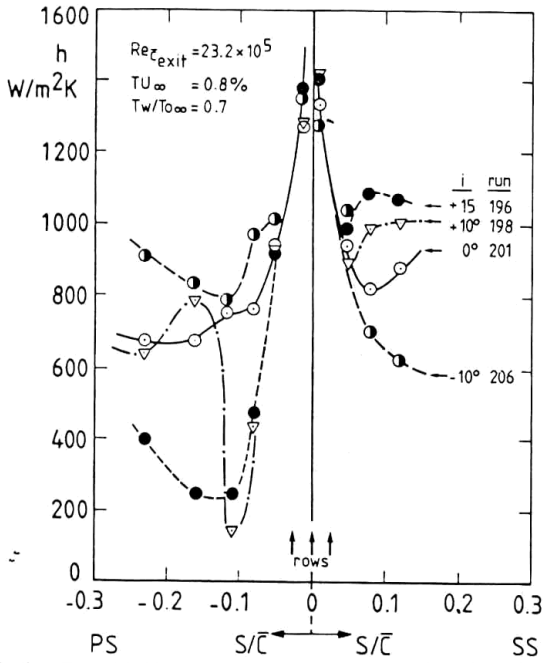

Fig. 6 Leading-edge heat transfer without cooling effect of incidence

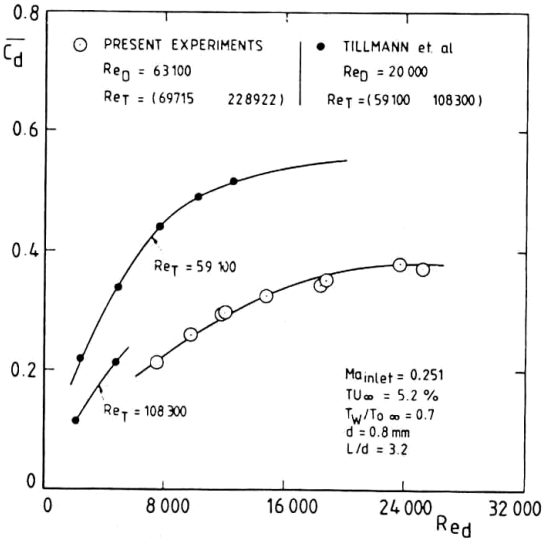

Fig. 7 Cooling holes discharge coefficients

of the three-dimensional vortices originating from the stagnation region may occur [16], due to the unfavorable pressure gradient (Fig. 2). Along the suction side a definite influence of the holes is observed on the transition process. The data obtained on the smooth blade demonstrate the relationship existing between turbulence intensity (3.0 . . . 5.2 percent) and transition onset and length (Fig. 4). Measurements on the present model suggest a very early transition induced by the presence of the cooling holes: the suction-side boundary layer appears to be fully turbulent at $s/\bar{c} = 0.25$. As already shown by other investigators [17, 18] free-stream turbulence variations only affect laminar or transitional boundary layers in the presence of a favorable pressure gradient in a significant way as shown in Fig. 4 for $-0.01 < s/\bar{c} < 0.20$.

Leading-Edge Heat Transfer Without Film Cooling ($i \neq 0$ deg). Leading-edge velocity distributions and stagnation point location were computed at different incidences using a Martensen method (Fig. 5). The corresponding heat transfer

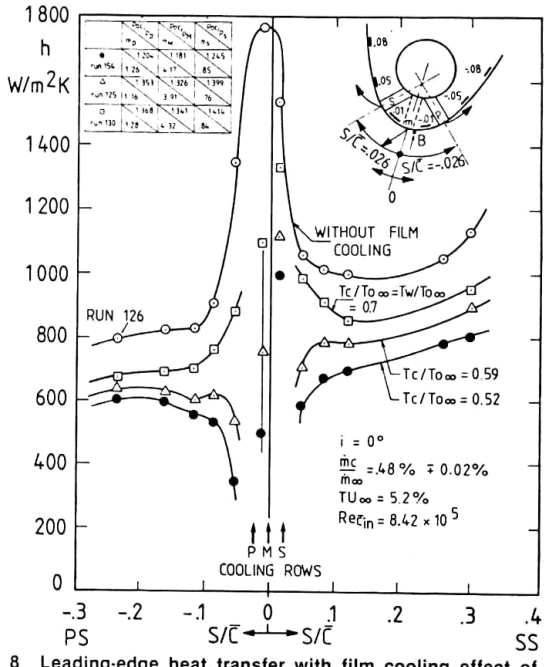

Fig. 8 Leading-edge heat transfer with film cooling effect of temperature ratio

evolutions are presented in Fig. 6. At zero incidence, as a result of the tripping effect of rows M and S, the onset of suction-side boundary layer transition is observed at $s/\bar{c} = 0.08$. In this paper, we have defined the onset of transition location to be the first measurement point where h starts to increase in a pronounced way. Increasing the incidence to +10 deg and +15 deg moves the stagnation point respectively to points A and D whereas transition onset is displaced to $s/\bar{c} = 0.065$ and 0.050. At $i = -10$ deg, the stagnation point is located in C and only row S disturbs the suction-side boundary layer. On the pressure side, at $i = 0$ deg and $i = -10$ deg, transition is observed to occur at $s/\bar{c} = -0.08$, because of the adverse pressure gradient. In the latter case, a higher local free-stream velocity level, enhancing local Re number as well as the disturbing effect of rows M and P, is responsible for slightly higher heat transfer coefficient values. At $i = +15$ deg, the stagnation point D nearly coincides with row P and the unfavorable pressure gradient almost disappears; hence larger laminar and transitional regimes are expected. This behavior has been confirmed by the measurements (Fig. 6).

Leading-Edge Heat Transfer With Film Cooling ($i = 0$ deg). Because of different free-stream conditions around the leading edge, as well as different internal flows, the local discharge coefficients of the three rows differ from each other; moreover, local mass flow rate measurements through each row were not possible. As a result, a mean discharge coefficient $\overline{C_d}$ was evaluated from the total coolant mass flow rate, the coolant plenum total pressure as well as an averaged free-stream static pressure. The $\overline{C_d}$ distribution, obtained for a mass weight ratio range of 0.48 to 1.01 percent, is shown in Fig. 7. The present data show qualitative agreement with measurements obtained in a water tunnel on a cylinder with three cooling rows by Tillman et al. [19].

The effect of coolant temperature on the convective heat transfer coefficient distribution is shown in Fig. 8. The coolant to free stream temperature ratio was varied from 0.5 to 0.7 for a constant mass weight ratio of 0.48 percent. From stagnation point location predictions as well as from qualitative oil flow visualizations, it appears that the suction-side wall heating is affected by the coolant jets from rows M

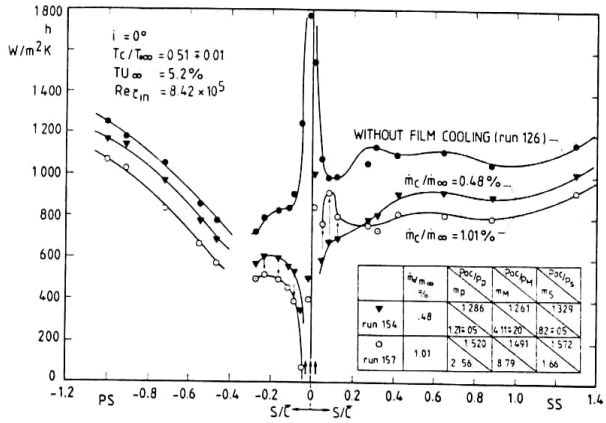

Fig. 9 Leading-edge heat transfer with film-cooling effect of mass weight ratio

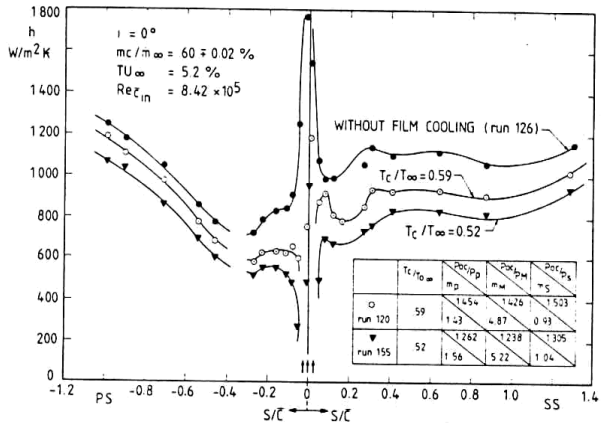

Fig. 10 Leading-edge heat transfer with film cooling

and S, whereas the pressure-side heat flux is only affected by row P.

The blowing rate m has been the most documented parameter in film-cooling research because of its governing role in the distribution of coolant fluid inside the viscous layers, normal to the wall. A given distribution establishes its specific mean velocity gradients and the associated turbulent shear stress and turbulent kinetic energy distributions. Unfortunately, because of a lack of detailed static pressure measurements, a very accurate determination of local m values was not obtained. An attempt to calculate local m values was made using the calculated local isentropic coolant mass flux rate, the averaged $\bar{C}_d$ and the predicted free-stream mass flux rate. Looking at Fig. 8, local blowing rate values of 4.17, 1.26, and 0.85 were respectively obtained for rows M, P, and S. On the suction side, highly penetrating jets from row M disturb the approaching mainstream boundary layer; downstream of this row, a separated coolant layer zone is observed ($s/\bar{c} = 0.01$), where a poor cooling efficiency is achieved. Reattachment is expected near row S due to the free-stream acceleration and strong convex curvature. Although this region does not seem to be submitted to the influence of a coolant film, the gauge located at $s/\bar{c} = -0.01$ provides a quite low heat transfer coefficient measurement. This observation may be attributed to the fact that, even with this low-conductivity material and short running times of the facility, local wall temperature measurements could be affected by conduction in between closely spaced ejection rows ($-0.01 < s/\bar{c} < +0.01$). This influence is mainly related with the local wall temperature measurement, rather than the wall heat flux measurement which is only sensitive to the time rate of change of wall temperature. The comparison of heat

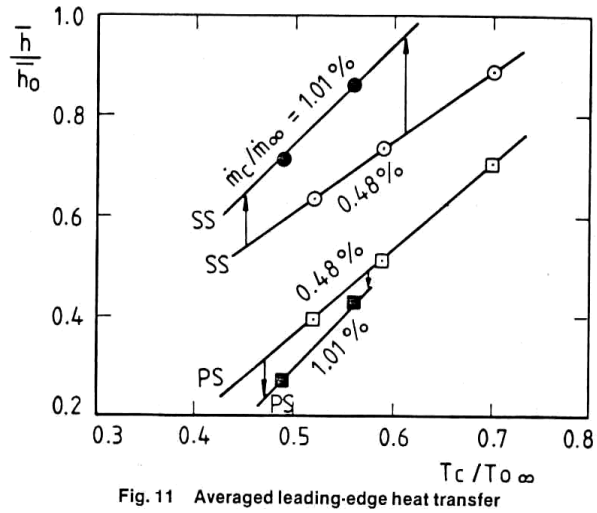

Fig. 11 Averaged leading-edge heat transfer

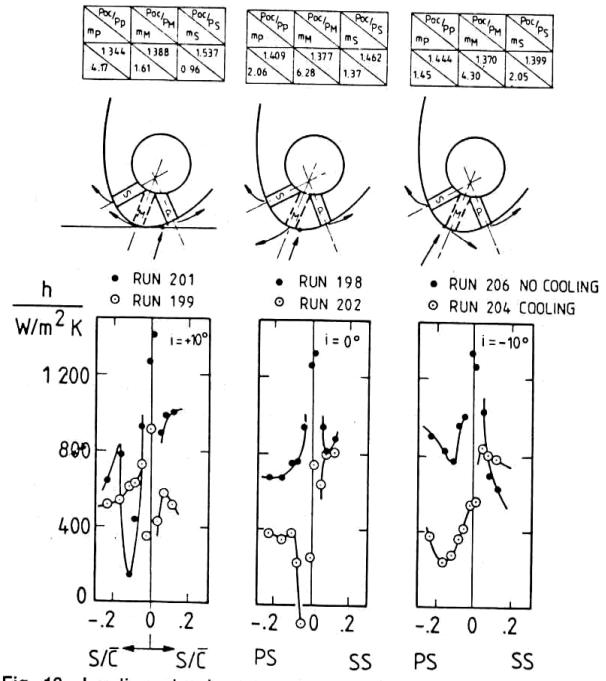

Fig. 12 Leading-edge heat transfer with film cooling, effect of incidence

transfer coefficients evaluated with an isothermal wall and with the locally measured wall temperatures displayed a quite negligible difference after three hole diameter downstream of rows P and S. In the showerhead region ($s/\bar{c} = \mp 0.01$), h measurement has some additional uncertainty because of the interrow heat conduction.

The effect of coolant mass weight ratio is shown in Fig. 9. This parameter was varied from 0.48 to 1.01 percent for a fixed value of coolant to free-stream temperature ratio of 0.51. Film cooling applied with a higher mass weight ratio provides a reduced heat transfer pattern along the pressure side. Although row P, ejecting along a concave surface, has a quite high blowing rate (2.56), the measured heat transfer pattern shows that the coolant remains attached to this concave surface, providing a correct wall protection. This behavior confirms the trends already observed in a low-speed environment [20]. For a high coolant mass weight ratio (1.01 percent), the blowing rate amounts to 8.79 across row M whereas a value of 1.66 is observed across row S. As might be expected, due to the high momentum flux of these jets, the

disturbed region is enlarged on the suction side and the reattachment point is moved more downstream. Behind row S, the first three gauges experience wall heat flux levels comparable to zero injection situation. From Fig. 9, there is experimental evidence that the jets ejected from row S separate from this convex surface. Coolant jet separation from convex surfaces at high blowing rates is, however, a well-known effect [20]. After reattachment, measured wall heat flux values far downstream ($s/\bar{c} > 0.25$) are lower than when moderate mass weight ratios (0.50 percent) are applied. In order to find the upper mass weight ratio limit before jet separation, heat transfer distributions were obtained for $\dot{m}_c/\dot{m}_\infty = 0.60$ percent and $T_c/T_{0\infty} = 0.52$ and 0.59 (Fig. 10). For the lowest coolant temperature ratio, the coolant ejected through row S is at the onset of separation: A slight heat transfer augmentation is observed only at $s/\bar{c} = +0.08$; the local blowing rates through rows M and S are respectively 5.22 and 1.04. Increasing the coolant temperature ratio, at an almost constant blowing rate, leads to a partially separated coolant flow situation. As a matter of fact, an increase of $T_c/T_{0\infty}$ results in a decrease of ρ_c/ρ_∞ and hence, at constant m, in an increase of U_c/U_∞ and moreover of the momentum flux ratio, leading to a more severe jet separation. On the pressure side, no coolant jet separation has been observed.

Although strong variations exit in this region, an attempt was made to define a leading edge heat transfer coefficient as a function of coolant mass weight ratio and coolant to free-stream temperature ratio (Fig. 11) using only four gauges located on both sides of the stagnation point B; $\bar{h}$ and $\bar{h}_0$ were obtained as arithmetical averages both on suction and pressure side. On an average basis, the cooling looks more effective on the pressure side than on the suction side. As the mass weight ratio increases, the suction side appears to be less protected because of jet separation. The strong influence of $T_c/T_{0\infty}$ is also demonstrated.

Leading-Edge Heat Transfer With Film Cooling ($i \neq 0$ deg). The effect of incidence variations upon leading-edge heat transfer in the presence of cooling was investigated for constant values of mass weight ratio, temperature ratio, and outlet Reynolds number. Results as well as estimated flow paths are given in Fig. 12 whereas aerodynamic predictions were given in Fig. 5. For $i = 10$ deg, the stagnation point is very close to row P. The ejection in such a low-velocity area provides a much higher local blowing rate (4.17) than at zero incidence ($m_p = 2.0$). On the pressure side the laminar region, observed between point A and $s/\bar{c} = -0.10$ without ejection, obviously disappears because of the disturbing nature of the coolant jets in the boundary layer. However, cooling along this surface is not as efficient as for the zero incidence configuration. The local blowing ratios across rows M and S are 1.61 and 0.96. The coolant layers provide a very efficient wall protection as a result of a very smooth coolant introduction into the suction-surface boundary layer.

For $i = -10$ deg, the position of the stagnation point (C) suggests that the suction surface boundary layer is only affected by jets issued from row S ($m_s = 2.05$). The cooling efficiency is rather poor, most probably because of a very small portion of fluid ejected through this row. Cooling of the pressure side through rows M and P provides heat transfer coefficient reductions to values equal to at least half of those obtained for the noncooled configuration in between C and $s/\bar{c} = -0.30$.

Conclusions

Convective heat transfer in the boundary layers developing around the leading edge of a H.P. turbine rotor blade has been investigated both in absence and presence of film cooling, using a sophisticated short-duration technique.

The quatitative wall heat transfer measurements documented the downstream development of the boundary layers as affected by the existence of the injection holes, even without coolant flow.

Important convective heat transfer reductions were obtained in the presence of cooling for realistic temperature ratios. It has been confirmed that a row situated on or very close to the stagnation point ejects at a relatively higher blowing rate, disturbing the downstream viscous layers in a more pronounced way.

Near hole external heat transfer coefficients were found to be slightly influenced from internal conduction paths, in between closely spaced cooling holes. However, the conduction pattern near the ejection site in the present low-conductivity model reveals much less significant flow of heat than that of the blade made of a conventional superalloy. This behavior provides some safety margin in wall temperature predictions, incorporating the heat transfer coefficients presented in this paper.

The effect of incidence variations on heat transfer with and without film cooling was interpreted with the aid of inviscid flow prediction methods. Predicted coolant trajectories were found to be consistent with the measured data.

References

1 Olsson, U., "Advanced Engine Technology and its Influence on Aircraft Performance," *J. of Aircraft*, Vol. 19, No. 5, May 1982, pp. 380-384.

2 Richards, B. E., "Heat Transfer Meaurements Related to Hot Turbine Components in the von Karman Institute Hot Cascade Tunnel," *Testing and Measurements Techniques in Heat Transfer and Combustion*, AGARD CP 281, May 1980.

3 Jones, T. V., Schultz, D. L., and Hendley, A. D., "On the Flow in an Isentropic Free Piston Tunnel," ARC R&M 3731, Jan. 1973.

4 Consigny, H., and Richards, B. E., "Short Duration Measurements of Heat Transfer Rate to a Gas Turbine Rotor Blade," ASME JOURNAL OF ENGINEERING FOR POWER, Vol. 104, No. 3, July 1983, pp. 542-551.

5 Schultz, S. L., and Jones T. V., "Heat Transfer Measurements in Short Duration Hypersonic Facilities," AGARD-ograph No. 165, Feb. 1973.

6 Ligrani, P. M., Camci, C., and Grady, M. S., "Thin Film Heat Transfer Gauge Construction and Measurement Details," VKI TM 33, Nov. 1982.

7 Schlichting, H., *Boundary Layer Theory* (7th ed.), McGraw-Hill, New York, 1979, pp. 714-715.

8 Kline, S. J., and McClintock, F. A., "Describing Uncertainties in Single Sample Experiments," *J. Mechanical Engin.*, Vol. 75, No. 1, Jan. 1953, pp. 3-8.

9 Arts, A., "Cascade Flow Calculations Using a Finite Volume Method," in *Numerical Methods for Flow in Turbomachinery*, VKI LS 1982-05, Apr. 1982.

10 Van Den Braembussche, R., "Calculation of Compressible Subsonic Flow in Cascades with Varying Blade Height," ASME JOURNAL OF ENGINEERING FOR POWER, Vol. 95, No. 4, Oct. 1973, pp. 345-351.

11 Kestin, J., and Wood, R. T., "The Mechanism Which Causes Free-Stream Turbulence to Enhance Stagnation Line Heat and Mass Transfer," *Heat Transfer*, Vol. 2, Elsevier, Amsterdam, 1970.

12 Sadeh, W. Z., Brauer, H. J., and Garrison, J. A., "Visualization Study of Vorticity Amplification in Stagnation Flow," Colorado State U., SQUID-CSU-1-PU, Oct. 1977.

13 Kestin, J., and Wood, R. T., "The Influence of Turbulence on Mass Transfer From Cylinders," ASME *Journal of Heat Transfer*, Vol. 93, No. 4, Nov. 1971, pp. 321-327.

14 Turner, A. B., "Local Heat Transfer Measurements on a Gas Turbine Blade," *J. Mech. Eng. Science*, Vol. 13, No. 1, 1971.

15 Colladay, R. S., "Turbine Cooling-Turbine Design and Application," NASA SP 2100, 1975.

16 Daniels, L. C., "Film Cooling of Gas Turbine Blades," Ph.D. Thesis, Oxford Univ. Eng. Lab. Report No. 1302/79, 1979.

17 Buyuktur, A. R., Kestin, J., and Maeder, P. F., "Influence of Combined Pressure Gradient and Turbulence on the Transfer of Heat From a Plate," *International Journal of Heat and Mass Transfer*, Vol. 7, 1964, p. 1175.

18 Junkhan, G. H., and Serovy, G. K., "Effects of Free-Stream Turbulence and Pressure Gradient on Flat Plate Boundary Layer Velocity Profiles and Heat Transfer," ASME *Journal of Heat Transfer*, Vol. 69, No. 2, May 1967, pp. 169-176.

19 Tillman, E. S., Hartell, E. L., and Jen, H. F., "The Prediction of Flow Through Leading Edge Holes in a Film-Cooled Airfoil With and Without Inserts," ASME Paper No. 84-GT-4, 1984.

20 Ito, S., Goldstein, R. J., and Eckert, E. R. G., "Film Cooling of a Gas Turbine Blade," ASME JOURNAL OF ENGINEERING FOR POWER, Vol. 100, No. 3, July 1978, pp. 476-481.

Printed in U.S.A.